11C.3 COMPARISON OF TECHNIQUES FOR ISOLATING EQUATORIAL ROSSBY WAVES IN SYNOPTIC STUDIES

Carl J. Schreck, III*
University at Albany, SUNY, Albany, NY

1. INTRODUCTION

Equatorial wave modes have been an increasing source of interest in recent years. However, isolating these waves in the intricacies of unfiltered tropical data can be difficult. Numerous studies have used a range of band-pass time filters to isolate these waves (Kiladis and Wheeler 1995; Dickinson and Molinari 2002; Molinari et al. 2006, manuscript submitted to *J. Atmos. Sci.*; and others). On the other hand, Wheeler and Kiladis (1999) and Roundy and Frank (2004) proposed methods for isolating these waves using a space-time filter.

Wheeler and Kiladis (1999) defined regions of the symmetric and anti-symmetric wavenumber-frequency domain to be associated with each wave mode based on their shallow water phase relation for small equivalent depths (8-90 m). Roundy and Frank (2004) suggested a slightly different method for isolating the waves. Notably, Roundy and Frank did not impose symmetry constraints in their filter, and they defined a larger region for n=1 equatorial Rossby (ER) waves that was less constrained by the shallow water phase relations.

The present study examines an ER wave packet using unfiltered, time-filtered, and space-time filtered data, with and without symmetry constraints. By investigating a single case using these varying techniques, the relative strengths and weaknesses of each method will be assessed.

2. DATA AND METHODOLOGY

This study focuses on an ER wave packet in the central Pacific during September, October, and November 1997. This packet is identified using twice-daily European Centre for Medium-Range Forecasting (ECMWF) uninitialized gridded analyses available on a 1.125° latitude-longitude grid. Furthermore, brightness temperature (T_b) data from the Cloud Archive User Service (CLAUS) on a global grid with 0.5° latitude-longitude and 3 h resolution is used as a proxy for tropical convection.

A 15-40 day band-pass filter is used for time filtering, following Molinari et al. (2006). Space-time filtering is performed following Wheeler and Kiladis (1999), both with and without the symmetry constraints.

3. RESULTS

Figure 1 is a Hovmöller of T_b averaged 10°S-10°N (shaded) and zonal wind component averaged 4.5°S-4.5°N (contoured). Filled hurricane symbols indicate tropical cyclogenesis between the equator and 10.5°N, and open symbols denote events south of the equator to 10.5°S.

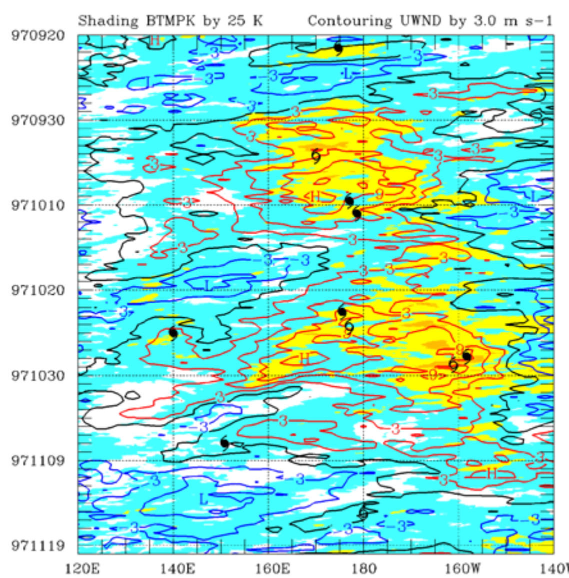

Fig.1: Hovmöller plot of unfiltered 850-hPa zonal wind component (contoured), averaged over 4.5°S-4.5°N, and unfiltered brightness temperature (shaded), averaged over 10°S-10°N, overlaid with tropical cyclogenesis locations for events that occurred 10.5°S-10.5°N. Zonal wind is contoured every 3 m s^{-1}, with negative contours in blue and positive contours in red. The zero contour is black. Brightness temperature less than 290 K is shaded in 25 K intervals. Filled in hurricane symbols represent northern hemisphere cyclogenesis events and open hurricane symbols represent southern hemisphere cyclogenesis events.

Corresponding author address: Carl J. Schreck, III, Department of Earth and Atmospheric Sciences, University at Albany, SUNY, Albany, NY 12222.
e-mail: carl@atmos.albany.edy

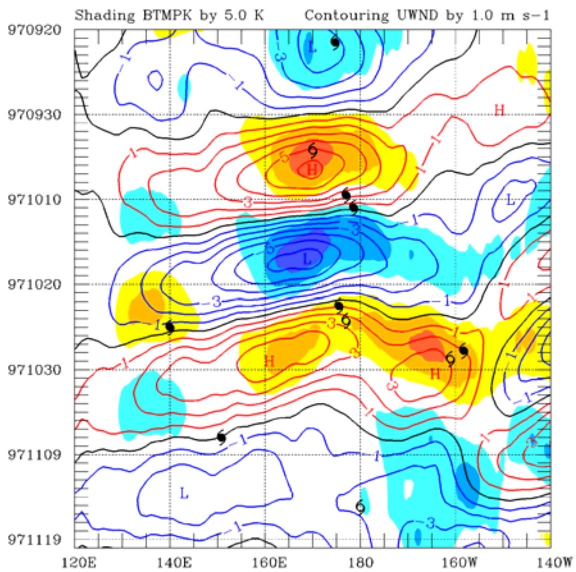

Fig. 2: Hovmöller plot of band-pass 15-40 day 850 hPa zonal wind component anomalies (contoured), averaged over 4.5°S-4.5°N, and band-pass 15-40 day brightness temperature (shaded), averaged over 10°S-10°N, overlaid with tropical cyclogenesis locations for events that occurred 10.5°S-10.5°N. Zonal wind anomalies are contoured every 1 m s-1, with negative contours in blue and positive contours in red. The zero contour is black. Brightness temperature anomalies are shaded in 5 K intervals, with anomalies less than -5 K shaded in warm colors and anomalies greater than 5 K shaded in cool colors. Filled in hurricane symbols represent northern hemisphere cyclogenesis events and open hurricane symbols represent southern hemisphere cyclogenesis events.

While Fig. 1 shows the complexity of unfiltered equatorial data, some structures may be discerned. Episodes of westerlies alternate with weaker westerlies or easterlies. Active convection and near-simultaneous tropical cyclogenesis in each hemisphere occur within and east of the westerlies.

Figure 2 shows a similar Hovmöller but for 15-40 day band-pass time filtered data. The oscillation of westerly wind and negative T_b anomalies with easterly wind and positive T_b anomalies shows more clearly. Twin tropical cyclogenesis remains associated with the westerly and negative T_b anomalies. The zonal wind anomalies show a mean westward propagation of -4.3 m s^{-1} and the group velocity is -0.5 m s^{-1}. The mean wavelength of the waves in Fig. 2 is 7500 km. Given that the background zonal wind is 2.6 m s^{-1}, these characteristics resemble a Doppler-shifted ER wave with an equivalent depth between 20 and 100 m.

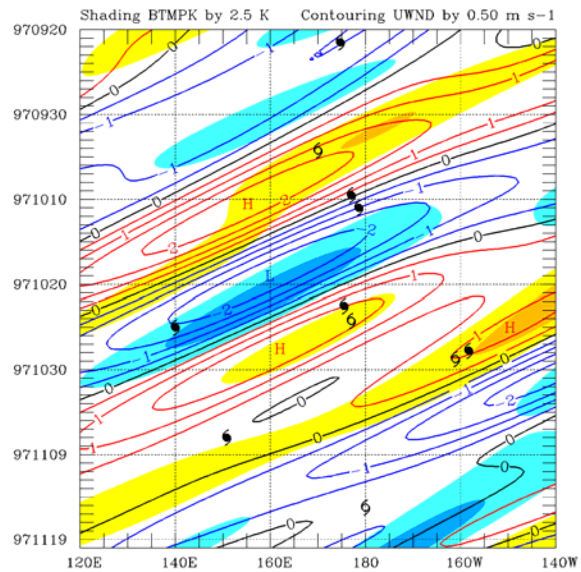

Fig. 3: As in Fig. 2, but for the space-time filtered zonal wind component (contoured) and space-time filtered brightness temperature (shaded). Zonal wind anomalies are contoured every 0.5 m s-1, with negative contours in blue and positive contours in red. The zero contour is black. Brightness temperature anomalies are shaded in 2.5 K intervals with anomalies less than –2.5 K shaded in warm colors and anomalies greater than 2.5 K shaded in cool colors.

Figure 3 is similar to Fig. 2, but using the Wheeler and Kiladis (1999) space-time filter. The general pattern is similar to the time-filtered data, but the westward propagation is more uniform. The space-time filtered waves propagate slightly faster with a phase velocity of -4.9 m s^{-1} and a group velocity of 0.2 m s^{-1}. The space-time filtered waves are also a bit longer with a wavelength of 7800 km.

Space-time filtered data (Fig. 3) shows very clearly propagating ER waves. However, the waves are much smoother and have smaller amplitude than in the other two datasets. As a result, important features of the waves may have been lost. The time-filtered data (Fig. 2) has larger amplitude, but the westward propagation is less clear and some eastward propagating features pass through the filter. A detailed discussion of the strengths and weaknesses of each method for studying equatorial waves and the importance of using these techniques in conjunction with each other will be presented in this talk.

4. ACKNOWLEDGEMENTS

This work was supported by National Science Foundation grant ATM-0513428, under the advisement of Dr. John Molinari. The time-filtering program was provided by Dr. Anantha Aiyyer, and the space-time filtering program was provided by Dr. George Kiladis and Dr. Matt Wheeler. Gridded analyses from the European Centre for Medium Range Weather Forecasts were obtained from the National Center for Atmospheric Research (NCAR), which is supported by the National Science Foundation. Cloud Archive User Service (CLAUS) data was provided by the British Atmospheric Data Centre and Dr. Kevin Hodges assisted in reading the data set.

5. REFERENCES

Dickinson, M., and J. Molinari, 2002: Mixed Rossby-gravity waves and western Pacific tropical cyclogenesis. Part I: Synoptic Evolution. *J. Atmos. Sci.*, **59**, 2183-2196.

Kiladis, G. N., and M. Wheeler, 1995: Horizontal and vertical structure of observed tropospheric equatorial Rossby waves. *J. Geophys. Res.*, **100** (D11), 22 981-22 997.

Molinari, J. M., K. Canavan, and D. Vollaro, 2006: Tropical cyclogenesis within an equatorial Rossby wave packet. Submitted to *J. Atmos. Sci.*

Roundy, P. E., and W. M. Frank, 2004: A Climatology of Waves in the Equatorial Region. *J. Atmos. Sci.,* **61**, 2105–2132.

Wheeler, M., and G. N. Kiladis, 1999: Convectively coupled equatorial waves: Analysis of clouds and temperature in the wavenumber-frequency domain. *J. Atmos. Sci.*, **56**, 374-399.